

# CatMaster: An Agentic Autonomous System for Computational Heterogeneous Catalysis Research

Honghao Chen, Jiangjie Qiu, Yi Shen Tew, and Xiaonan Wang\*

*Beijing Key Laboratory of Artificial Intelligence for Advanced Chemical Engineering Materials, Department of Chemical Engineering, Tsinghua University, Beijing, China*

E-mail: wangxiaonan@tsinghua.edu.cn

## Abstract

Density functional theory (DFT) is widely used to connect atomic structure with catalytic behavior, but computational heterogeneous catalysis studies often require long workflows that are costly, iterative, and sensitive to setup choices. Besides the intrinsic cost and accuracy limits of first-principles calculations, practical workflow issues such as keeping references consistent, preparing many related inputs, recovering from failed runs on computing clusters, and maintaining a complete record of what was done, can slow down projects and make results difficult to reproduce or extend.

Here we present *CatMaster*, a large-language-model (LLM)-driven agent system that turns natural language requests into complete calculation workspaces, including structures, inputs, outputs, logs, and a concise run record. CatMaster maintains a persistent project record of key facts, constraints, and file pointers to support inspection and restartability. It is paired with a multi-fidelity tool library that covers rapid surrogate relaxations and high-fidelity DFT calculations for validation when needed. We demonstrate CatMaster on four demonstrations of increasing complexity: an O<sub>2</sub> spin-state check with remote execution, BCC Fe surface energies with a protocol-sensitivity study and CO adsorption site ranking, high-throughput Pt–Ni–Cu alloy screening for

hydrogen evolution reaction (HER) descriptors with surrogate-to-DFT validation, and a demonstration beyond the predefined tool set, including equation-of-state fitting for BCC Fe and CO-FeN<sub>4</sub>/graphene single-atom catalyst geometry preparation. By reducing manual scripting and bookkeeping while keeping the full evidence trail, CatMaster aims to help catalysis researchers focus on modeling choices and chemical interpretation rather than workflow management.

## Introduction

Density functional theory (DFT) has established itself as an indispensable tool in heterogeneous catalysis, providing quantitative links between atomic structure, adsorption thermodynamics, and catalytic activity. However, practical catalysis studies are rarely reducible to single calculations. Even standard tasks such as determining surface energies or screening descriptors often require orchestrating multi-step workflows: selecting bulk references, constructing and relaxing slabs under consistent constraints, enumerating adsorption sites, and managing job submission queues.

While the community has developed robust libraries for atomistic simulations (e.g., ASE, pymatgen) and workflow managers for job orchestration,<sup>1–5</sup> a significant operational gap around the practical use of these libraries persists. Consequently, researchers still frequently rely on manual intervention to chain disparate tools, convert data formats, and track intermediate structures. This manual oversight requires too many micro-decisions: managing calculation files, adjusting convergence parameters, diagnosing failures, or selecting candidates for high-fidelity validation. This overhead may slow iteration and complicate the exploration of vast chemical spaces.

Large language model (LLM) agents offer a compelling interface for such workflows, enabling researchers to express protocol intent in natural language while the agent coordinates the underlying tools. Recent efforts in chemistry and materials science have demonstrated the feasibility of LLM-driven automation.<sup>6–10</sup> For rigorous catalysis research, however, three re-

quirements are particularly important: (i) *evidence-based execution*, ensuring the generation of inspectable artifacts (inputs, logs, reports); (ii) *robustness*, enabling reliable local project resumption following interruptions while supporting execution on remote HPC systems; and (iii) *auditability*, enabling the traceability of intermediate decisions for the long-running project.

CatMaster addresses these needs by treating the calculation workspace as the primary scientific record with a hierarchical agent system design. Instead of producing chat-only narratives, CatMaster organizes execution into milestone tasks with concrete deliverables, continuously serializes artifacts to disk, and maintains a persistent project record of key facts, constraints, and file pointers that downstream steps can consume. In this work, we make four contributions: (i) we introduce a file-centric execution contract that turns natural-language protocols into restartable, inspectable workspaces; (ii) we implement hierarchical agent orchestration with persistent whiteboard memory to support long-horizon workflows and deferred resolution of unknown intermediate outcomes; (iii) we demonstrate multi-fidelity catalysis screening that couples surrogate-scale exploration with targeted DFT validation; and (iv) we show tool-light compositional autonomy on long-tail tasks via controlled Python-based composition. This design ensures that a natural language request evolves into a shareable, restartable workspace, shifting the researcher’s focus from manual maintenance to high-level modeling choices and mechanistic insights.

## Results and Discussion

### Overall workflow

CatMaster is aimed at atomistic catalysis research where scientific questions are posed at the project level (e.g., “screen HER candidates”), yet execution involves coupled steps and iterative refinement. Rather than merely automating scripts, CatMaster emphasizes three deliverables that are critical for rigorous research: (i) a self-contained workspace that houses

all structures, inputs, outputs, and analysis scripts; (ii) resilience to interruption, enabling seamless project resumption across local and remote resources; and (iii) full traceability, allowing protocol decisions and derived quantities to be audited and revised.

We treat the workspace as an execution contract: each milestone task is expected to emit a minimal evidence package, including the relevant input decks, output logs, and a machine-readable summary of key scalars, together with a persistent record entry that enables downstream tasks to resolve dependencies without relying on chat context. The overall workflow is illustrated in Figure 1. A user request is decomposed into milestone tasks by the Planner (with optional human review). The Executor (Taskrunner and Tasksummarizer) then orchestrate domain-specific tools for structure manipulation, data retrieval, and analysis, dispatching calculations across heterogeneous resources ranging from local preprocessing to GPU-accelerated surrogate models and HPC-based DFT operations. Throughout execution, CatMaster continuously serializes artifacts and updates a compact project record, ensuring that workflows remain inspectable and restartable independent of the conversational context.

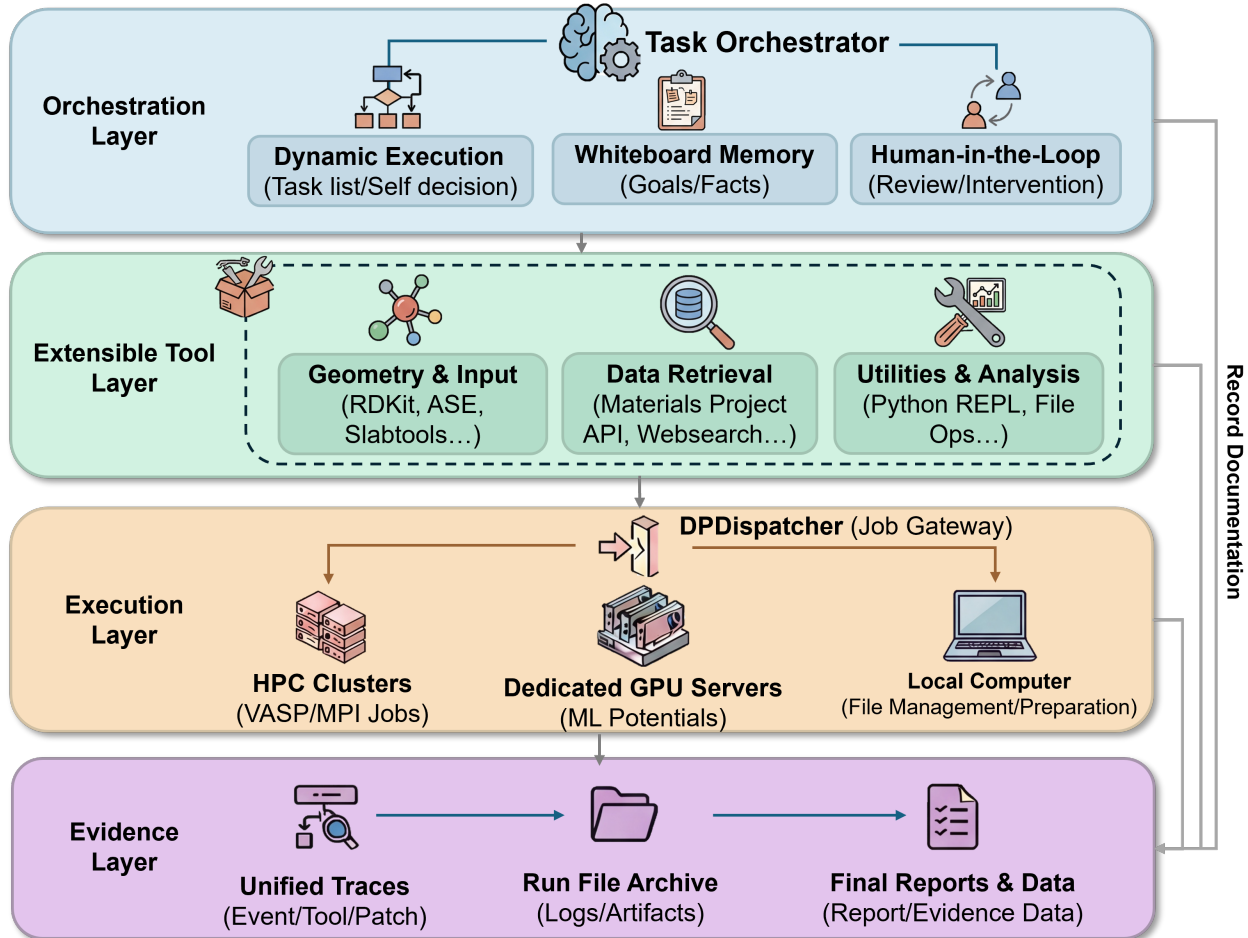


Figure 1: Overview of CatMaster’s architecture and file-centric data lineage. A high-level protocol request is decomposed into milestone tasks by the orchestration layer (dynamic execution, persistent whiteboard memory, and optional human-in-the-loop checkpoints). These tasks are executed through an extensible tool layer (geometry/input, data retrieval, and analysis utilities) and dispatched to heterogeneous compute backends (HPC clusters, dedicated GPU servers, and local resources). A unified evidence layer archives traces, artifacts, and final reports to support inspection, reproducibility, and restartability.

## Hierarchical agent orchestration: The O<sub>2</sub> “Hello World” case study

The oxygen molecule (O<sub>2</sub>) in a vacuum box serves as a canonical introductory example for electronic structure theory and the first practical tutorial in the official VASP documentation.<sup>11</sup> We utilize this classic case to illustrate the internal lifecycle of a CatMaster workflow. This study demonstrates how the system translates a high-level intent into concrete tool execution.

The workflow begins with a specific natural language request from the user. The prompt was: “I need you to compare the singlet and triplet O<sub>2</sub> in a box: Prepare VASP inputs from scratch, perform VASP calculation... and report final energy per atom and O–O bond distance.”

The **Planner** analyzed this request. It decomposed the intent into a linear sequence of seven distinct milestone tasks and executed the following structured plan:

1. **Workspace Setup:** The agent created a clean directory tree for the project.
2. **Geometry Generation:** It built the 3D O<sub>2</sub> structure from the SMILES string “O=O” and centered it within a cubic periodic box.
3. **Input Preparation:** The agent generated standard VASP relaxation inputs using the `relax_prepare` tool.
4. **Spin Constraint Enforcement:** A dedicated task modified the INCAR files. This step explicitly defined the singlet and triplet spin states.
5. **Batch Execution:** The agent submitted the calculations using `vasp_execute_batch`. This ensured efficient handling of the jobs.
6. **Post-processing:** Upon completion, the agent parsed the OUTCAR and CONTCAR files. It extracted the final energies and bond lengths.
7. **Reporting:** The final task synthesized these findings into a Markdown summary file.

It is important to note that the Planner does not rigidly bind tasks to specific tool calls. Instead, it defines tasks as logical milestones. This design decouples high-level intent from low-level execution. It allows the Task Runner to autonomously handle micro-decisions without cluttering the main plan. Simultaneously, it ensures the overall workflow remains clear and readable for human review.

The Task Runners sequentially executed each step in this workflow, expanding tasks into 40 total tool calls with 12 unique tools. They verified intermediate deliverables, such

as the existence of POSCAR files and convergence markers. Figure 2a visualizes this linear execution flow. The agent correctly identified the triplet state as the ground state. It reported an energy difference of 0.38 eV. Both states relaxed to chemically sensible bond lengths (1.233–1.234 Å)(Figure 2b). This successful validation serves as a foundational proof-of-concept for CatMaster’s design and demonstrates that CatMaster can autonomously bridge the gap between abstract chemical intent and rigorous, verifiable evidence.

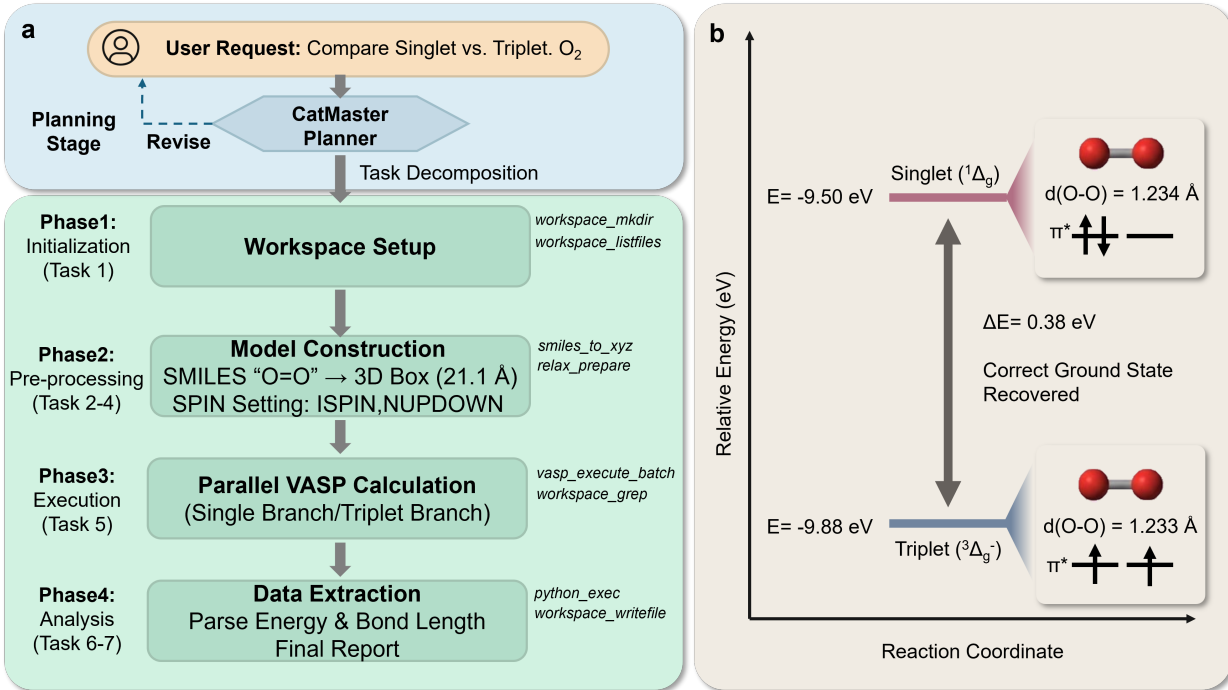


Figure 2: Lifecycle of the O<sub>2</sub> spin-state workflow illustrating CatMaster’s sequential execution and evidence generation. (a) Milestone task sequence produced by the Planner and executed by the tool layer, including workspace setup, molecular construction, VASP input preparation, parallel execution of singlet/triplet branches, and automated parsing/reporting. (b) Scientific artifact from the run: the triplet state is recovered as the ground state, with  $\Delta E_{\text{singlet-triplet}} = +0.38$  eV (PAW-PBE) and chemically sensible relaxed O–O bond lengths.

## BCC Fe surface chemistry: From validation to autonomous exploration

We selected the surface chemistry of BCC Fe as a representative case to evaluate two critical capabilities: (1) the accuracy of the agent against established benchmarks using standard

protocols, and (2) the agent’s ability to strictly adhere to user-imposed constraints during a multi-stage, end-to-end exploration.

### Validation against standard benchmarks.

First, to establish a baseline for physical correctness, CatMaster was tasked with computing surface energies for Fe(110), (100), and (111) using a standard protocol (symmetric slabs, PBE functional, no dispersion). The agent autonomously retrieved the correct bulk reference (`mp-13`), performed lattice relaxation, and constructed symmetric models. As shown in Table 1, the computed surface energies ( $\gamma_{110} = 2.48$ ,  $\gamma_{100} = 2.56$ ,  $\gamma_{111} = 2.76$  J/m<sup>2</sup>) align closely with literature values, with relative errors within 3%. This confirms that the agent can autonomously instantiate and execute a standard thermodynamic workflow with high accuracy.

Table 1: BCC Fe surface energies comparison between CatMaster (Standard Protocol) and literature references. Values in parentheses denote relative errors:  $(\gamma_{\text{ours}} - \gamma_{\text{ref}})/\gamma_{\text{ref}}$ . The close agreement validates the agent’s autonomous geometry handling and parameter selection. All values in J/m<sup>2</sup>.

Facet	CatMaster	Heiniger <sup>12</sup>	Tan <sup>13</sup>	MP <sup>5</sup>
(110)	2.48	2.56 (-2.98%)	2.46 (+0.96%)	2.45 (+1.50%)
(100)	2.56	2.63 (-2.48%)	2.50 (+2.59%)	2.50 (+2.63%)
(111)	2.76	2.80 (-1.41%)	2.73 (+1.12%)	2.73 (+1.12%)

### Context-aware planning with deferred resolution.

Real-world research often necessitates deviations from standard community recipes to test specific hypotheses. To evaluate CatMaster’s flexibility, we issued a second, more complex request: *”Compute Fe surface energies using center-fixed slabs and D3 dispersion corrections, then use the most stable 2x2 surface to identify the best CO adsorption site.”* Unlike the validation run, this task required the agent to translate explicit user constraints into precise input modifications—specifically, altering the selective dynamics and DFT-D3 setting tags rather than relying on retrieved parameter sets.

CatMaster faithfully executed this constrained protocol. As illustrated in Figure 3b, the inclusion of dispersion corrections and fixation constraints resulted in systematically higher surface energies ( $\sim +0.6 \text{ J/m}^2$ ) compared to the standard baseline. Crucially, this deviation represents a correct physical consequence of the imposed modeling choices rather than a computational error. The agent successfully calculated these shifted values while preserving the correct stability ranking ( $110 < 100 < 111$ ), demonstrating that it operates as a faithful executor of the user’s specific intent.

Beyond execution fidelity, this workflow highlights a key architectural feature: the ability to plan for unknown intermediate outcomes. At the initial planning stage, the identity of the “most stable surface” was undetermined. Rather than halting for human input, the Planner constructed a linear 18-step plan using logical placeholders and inter-task data contracts (Figure 3a). Specifically, the agent designated Task 11 to identify the stable facet and serialize the decision to a whiteboard artifact. Subsequent tasks (Tasks 13–17) were pre-configured to resolve their input geometry dynamically by reading this artifact. This mechanism of deferred resolution allowed CatMaster to define a long-horizon workflow containing conditional dependencies within a deterministic task list, effectively bridging the gap between static planning and dynamic execution. In particular, in subsequent relaxations of CO adsorption on the Fe(110)  $2\times 2$  slab, several nominally distinct initial placements (e.g. `bridge_0` and `bridge_1`) converge to the same relaxed on-top adsorption motif (Figure 3c), and the relaxed on-top geometry is the lowest-energy configuration among the tested initial structures.

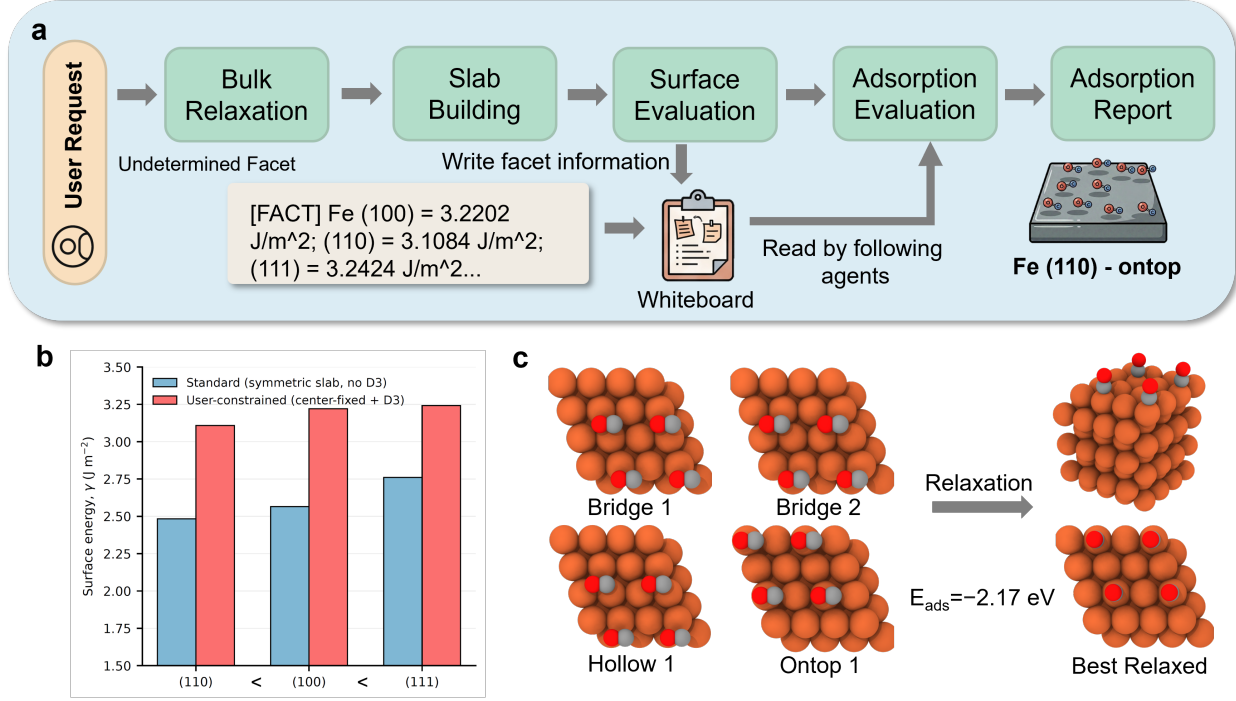


Figure 3: BCC Fe surface workflow: protocol sensitivity and downstream CO adsorption. (a) Deferred-resolution planning via a whiteboard data contract: the most stable facet is unknown at plan time and is written to a persistent record after surface evaluation, then consumed by subsequent adsorption tasks. (b) Protocol sensitivity of  $\text{Fe}(110)/(100)/(111)$  surface energies: comparison between a standard symmetric-slab protocol (no D3) and a user-constrained protocol (center-fixed slabs + D3), showing a systematic increase in  $\gamma$  while preserving the stability ordering. (c) CO adsorption relaxations on the  $\text{Fe}(110) 2 \times 2$  slab: representative initial placements (bridge/hollow/on-top) are relaxed, and multiple initial placements converge to a common relaxed on-top motif; the final relaxed configuration shown has  $E_{\text{ads}} \approx -2.17 \text{ eV}$ .

## Scale-out orchestration: Multi-fidelity HER screening in Pt–Ni–Cu alloys

Moving beyond single-system benchmarks, we tasked CatMaster with a project-level challenge: orchestrating a high-throughput, multi-fidelity screening campaign for hydrogen evolution reaction (HER) catalysts in the Pt–Ni–Cu alloy space. The user explicitly requested a funnel-like pipeline: retrieving candidates, generating a vast library of adsorption sites, performing rapid pre-screening with a machine learning surrogate (MACE), and identifying top candidates for targeted high-fidelity DFT validation.

To initiate this workflow, CatMaster autonomously navigated the Materials Project database for binary and ternary combinations of Pt, Ni, and Cu. It applied a stability filter ( $E_{\text{hull}} < 0.05$  eV) as requested by the user, identifying ten candidates (5 Pt–Ni, 3 Pt–Cu, 2 Ni–Cu) which were deduplicated to eight distinct compositions, including phases such as  $\text{Cu}_3\text{Pt}$ , NiPt, and  $\text{CuPt}_7$ . From this pool, the agent constructed a diverse structural library of 35 slab models across low-index facets ((100)/(110)/(111)), standardizing them with a 12 Å slab thickness and 15 Å vacuum by default. To capture the full chemical complexity of these alloy surfaces, it enumerated 347 symmetry-unique hydrogen adsorption sites, covering diverse local environments including atop, bridge, and 3-/4-fold hollow sites using pymatgen.

Following the user’s multi-fidelity protocol, the agent deployed the MACE surrogate model to execute a massive batch of 383 relaxations (comprising 35 bare slabs, 347 adsorbed systems, and the  $\text{H}_2$  reference). (Figure 4a) This high-throughput execution enabled the agent to rank all 347 sites by the theoretical HER activity descriptor ( $\Delta G_{\text{H}^*} = \Delta E_{\text{H}^*} + 0.24$  eV), effectively filtering the search space before engaging expensive quantum mechanical resources.

Based on the surrogate ranking, the agent identified candidates clustering near the thermoneutral peak ( $\Delta G_{\text{H}^*} \approx 0$ ) and automatically triggered targeted DFT validation for the top four distinct cases (Figure 4b). The results (Table 2) highlight the **Cu<sub>3</sub>Pt(100)** surface at the `bridge_0` site as the most promising candidate site, with a DFT-computed  $\Delta G_{\text{H}^*}$  of  $-0.038$  eV. The validation step revealed surrogate errors ranging from  $+0.033$  to  $-0.149$  eV (Figure 4c), with the best candidate showing a remarkable agreement (MACE deviation of only  $+0.033$  eV). This outcome underscores the value of the agent’s multi-stage architecture: it leveraged MACE to discard the majority of the search space at low cost while autonomously reserving rigorous DFT verification for the final, critical decision-making step.

Table 2: Top HER candidates identified by the MACE surrogate screening and validated by DFT. Candidates were prioritized by their proximity to  $\Delta G_{H^*} \approx 0$ .

Candidate	Site	$\Delta G_{H^*}^{\text{MACE}}$ (eV)	$\Delta G_{H^*}^{\text{DFT}}$ (eV)	Error (eV)
Cu <sub>3</sub> Pt (100)	bridge_0	-0.0046	-0.0377	+0.0331
Cu <sub>3</sub> Pt (110)	bridge_0	+0.0050	-0.0933	+0.0983
NiPt <sub>3</sub> (110)	bridge_4	+0.0094	+0.0999	-0.0904
CuPt <sub>7</sub> (110)	bridge_7	-0.0012	+0.1481	-0.1493

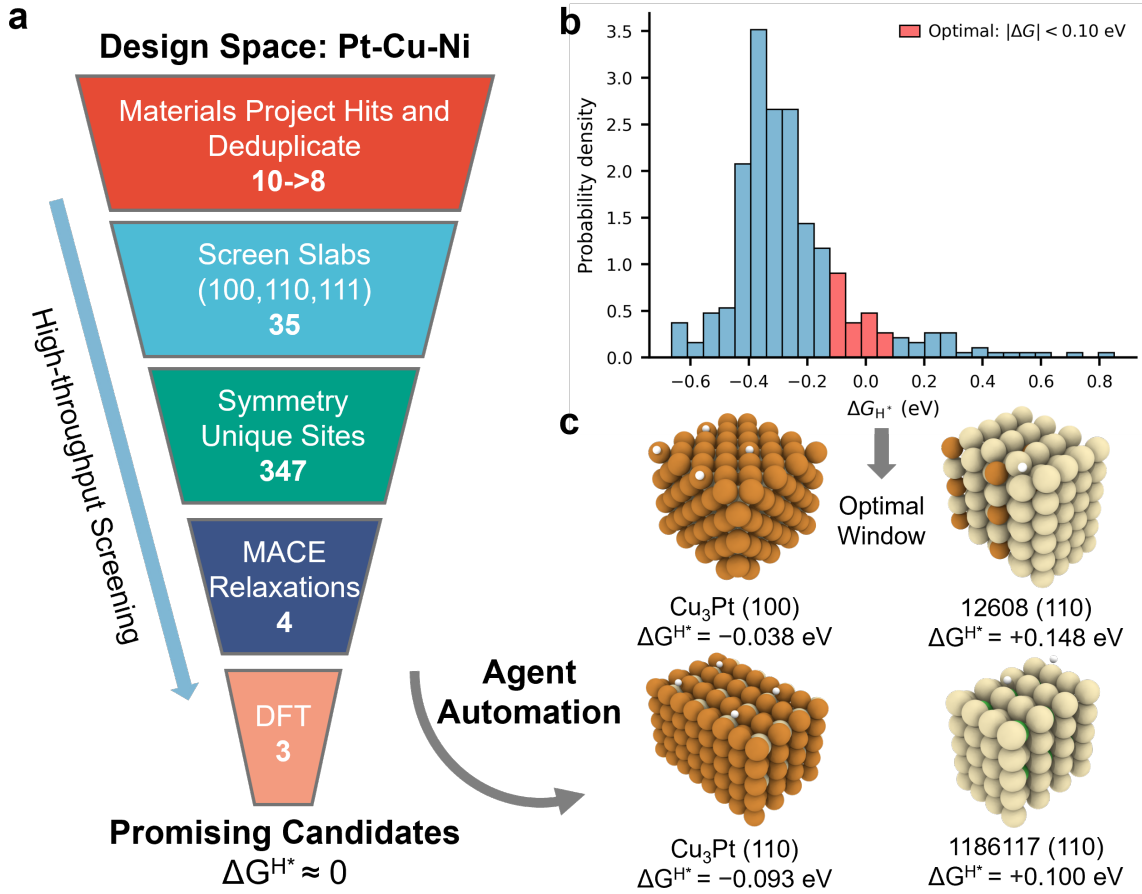


Figure 4: Outcomes of the multi-fidelity HER screening campaign in the Pt–Cu–Ni alloy space. (a) Funnel view of the pipeline from Materials Project retrieval and deduplication to slab generation, symmetry-unique adsorption-site enumeration, surrogate screening, and targeted DFT validation; numbers indicate the counts at each stage in this workflow run. (b) Distribution of  $\Delta G_{H^*}$  over all enumerated sites predicted by the surrogate, with the thermoneutral activity window highlighted (example criterion:  $|\Delta G| < 0.10$  eV). (c) Representative shortlisted candidate surfaces near the thermoneutral window (structures shown) with their validated  $\Delta G_{H^*}$  values.

## Bridging the long tail: Tool-light composition and procedural construction

A persistent challenge in autonomous computational science is the “long tail” of various tasks that are too niche to maintain the development of dedicated, hardened tools. Standard agents often struggle when they encounter a task outside their predefined toolset. CatMaster addresses this limitation not by expanding the tool library indefinitely, but by leveraging the LLM’s internal knowledge to create composition of stable *primitives* (basic tools), such as workspace I/O, batch execution hooks, and standard Python libraries for material applications, into novel scientific workflows. In the following two small demonstrations, we illustrate how CatMaster can (i) perform equation-of-state (EOS) fitting and (ii) reproduce CO adsorption on FeN<sub>4</sub>/graphene using MACE, despite the absence of dedicated, task-specific tools.

### Compositional autonomy: equation of state without dedicated tools

A good ablation study for CatMaster is fitting the equation of state for a specific material. Unlike specialized materials workflows that rely on pre-compiled routines for equation-of-state calculations, CatMaster possesses no specific tool for this task. Instead, the agent demonstrated compositional autonomy by logically decomposing the physical requirement into a sequence of generic operations. The agent first designed an isotropic volume scan experiment ranging from 8.0 to 16.0 Å<sup>3</sup>/atom across 41 distinct points using pymatgen itself. To execute this plan, it utilized the standard `relax.prepare` tool but correctly identified the need for static energy calculations rather than ionic relaxations. Consequently, it explicitly overrode the default VASP parameters by setting `NSW=0` and `IBRION=-1` to prevent ionic movement during the volume sweep. Following the successful batch execution of these 41 jobs, the agent wrote and executed a custom Python script using `numpy` and `scipy` to parse the resulting energies and fit them to the Birch–Murnaghan equation shown in Figure 5. The resulting fit yielded an equilibrium volume of  $V_0 = 11.41 \text{ \AA}^3/\text{atom}$  and a bulk modulus

of  $B_0 = 175.9$  GPa. This workflow confirms that the agent can effectively “invent” valid physical protocols by dynamically recombining generic computational primitives.

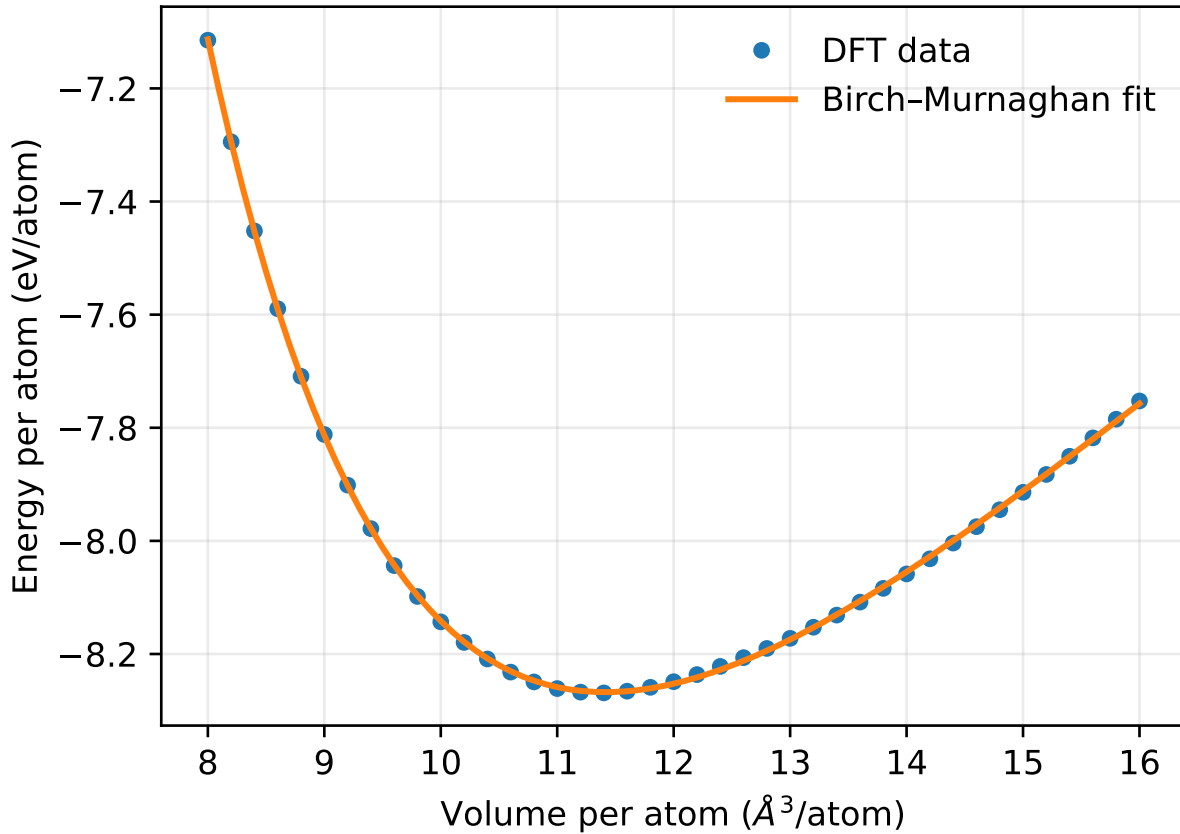


Figure 5: Equation-of-state (EOS) of BCC Fe generated via CatMaster using a volume scan. Markers denote DFT total energies as a function of volume per atom, and the solid line shows the Birch–Murnaghan fit used to extract the equilibrium volume and bulk modulus.

### Procedural structural construction: $\text{FeN}_4$ /graphene SAC

While bulk crystals are typically retrieved from databases, complex heterogeneous interfaces like Single-Atom Catalysts (SACs) often require manual construction in graphical interfaces. CatMaster demonstrates procedural construction capabilities by translating the abstract chemical concept of an “ $\text{FeN}_4$  site on graphene” into precise atomic manipulations without a dedicated retrieval tool (Figure 6). Lacking a pre-existing SAC template, the agent applied its internal chemical knowledge to edit a provided pristine graphene lattice using generic

Python scripting. The process began with the generation of a  $5 \times 5$  graphene supercell to create enough space for vacancy construction and active site building. The agent then engineered the defect by creating a divacancy—removing two central carbon atoms—and substituting four rim carbon atoms with nitrogen to form the pyridinic  $\text{N}_4$  pocket. An iron atom was placed at the pore center with an initial vertical offset of 1.5 Å relative to the graphene plane to avoid unphysical overlap. This constructed  $\text{C}_{44}\text{N}_4\text{Fe}_1$  geometry was subsequently smoothed via a fast MACE relaxation, converging in 37 steps to a maximum force below 0.05 eV/Å. To complete the catalytic model, the agent generated a CO molecule from its SMILES string (“C#O”) and procedurally docked it onto the metal center. The adsorbate was aligned along the surface normal in a C-down configuration with an initial Fe–C distance of 1.80 Å. Following a second MACE optimization of the full adsorbate–substrate complex, the workflow produced chemically sensible geometries, verifying that the agent’s conceptual understanding of the  $\text{FeN}_4$  topology was correctly translated into Cartesian coordinates through code generation.

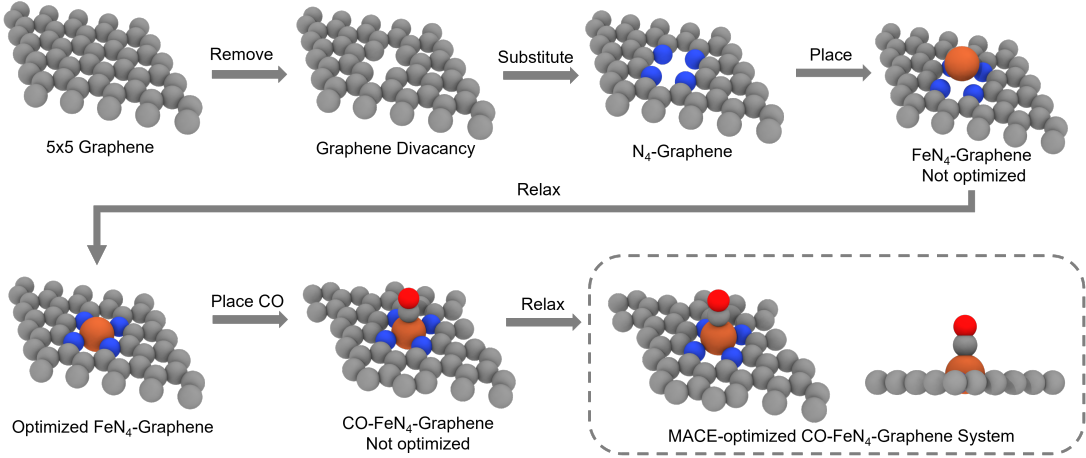


Figure 6: Procedural construction of an  $\text{FeN}_4$ /graphene single-atom catalyst and CO adsorption using generic structure-editing operations. Starting from a  $5 \times 5$  graphene supercell, a divacancy is created (Remove), four rim carbon atoms are substituted by N to form an  $\text{N}_4$  pocket (Substitute), and an Fe atom is placed at the site center (Place) to generate an initial  $\text{FeN}_4$ -graphene structure, followed by relaxation. CO is then placed in a C-down configuration on the Fe site and relaxed, yielding the optimized  $\text{CO@FeN}_4$ -graphene geometry (final system shown in top and side views).

## Limitations and Future Directions

While CatMaster demonstrates significant potential in automating catalysis workflows, several limitations remain that define the boundary between current capabilities and fully autonomous discovery.

**Execution vs. Scientific Reasoning.** CatMaster is currently designed as a rigorous execution and evidence-management layer, not a theoretical reasoning engine. It focuses on translating user intent into reliable computational actions but lacks a literature-grounded reasoning module. Consequently, it cannot yet autonomously critique methodological choices—such as selecting the appropriate exchange-correlation functional, determining magnetic ordering strategies, or justifying dispersion corrections—based on prior art. Scientific interpretation and the validation of physical protocols remain the responsibility of

human researchers. Future integrations with retrieval-augmented generation (RAG) systems capable of digesting academic literature could bridge this gap, enabling the agent to propose and justify method parameters.

**Linear Planning vs. Dynamic Adaptation.** Although the system successfully manages data dependencies through whiteboard-based "deferred resolution" (as seen in the Fe adsorption study) with an automatic human-in-the-loop mechanism that may allow user to alter a whole new task planning chain, the underlying planning architecture remains fundamentally linear. The current approach relies on a deterministic sequence of tasks where placeholders are resolved at runtime. This "linear-with-reference" model is sufficient for standard high-throughput screening but lacks the resilience of true dynamic graph execution. It may not yet handle complex, non-deterministic research paths where the *topology* of the workflow itself must adapt to intermediate findings (e.g., "*if surface reconstruction occurs, switch to a global optimization algorithm*"). Future iterations will move towards Directed Acyclic Graph (DAG) orchestration with conditional branching logic to support such adaptive research strategies.

**Risks of Generative Tool Composition.** The flexibility of LLM-driven science introduces distinct reliability risks, particularly when relying on the model's internal knowledge for tool composition and procedural geometry construction. As illustrated in the FeN<sub>4</sub> case, the agent's ability to construct valid geometries depends entirely on the chemical knowledge accuracy of its training data. Hallucinations or conceptual errors could theoretically lead to plausible-looking but chemically invalid structures (e.g., incorrect coordination environments) that generic relaxation tools might not correct. Balancing open-ended flexibility with rigorous validation layers—such as graph-based connectivity checks or reference-motif matching—is a critical frontier for ensuring robustness.

**Depth of Error Recovery.** Finally, while CatMaster handles low-level workflow exceptions (e.g., job resubmission or file handling errors), it currently lacks the "intuition" required for deep electronic structure troubleshooting. Complex failures typical in transition

metal catalysis, such as persistent SCF non-convergence, magnetic moment collapse, or geometry optimization oscillation, often require nuanced parameter adjustments (e.g., mixing schemes, pre-conditioning) that exceed the current agent’s capabilities. Developing specialized ”debugger agents” trained on large datasets of failed VASP calculations represents a necessary step toward truly unattended operation.

## Conclusions

CatMaster is an LLM-driven orchestration system for heterogeneous catalysis computations designed around a file-centric execution contract. By decomposing natural-language protocol requests into milestone tasks with concrete deliverables, executing through schema-validated tools, and persisting a lightweight project record of key facts and file pointers, CatMaster produces restartable and auditable workspaces rather than ephemeral chat-only narratives. Across workflows spanning spin-state checks, surface thermodynamics with protocol sensitivity, adsorption exploration, multi-fidelity HER screening with targeted DFT validation, EOS fitting, and procedural single-atom catalyst geometry construction, CatMaster generates evidence packages that can be inspected, rerun, and extended. We anticipate that this design can reduce manual workflow overhead while keeping computational outputs transparent and scientifically auditable.

## Methods

### Hierarchical architecture for CatMaster agents

CatMaster is architected for project-style catalysis computations where the primary deliverable is not merely a narrative response, but a reusable workspace containing structures, input decks, calculation outputs, and post-processing scripts. Figure 1 summarizes the core philosophy: while the LLM serves as the orchestration layer, the authoritative project state

is persisted in the file system rather than the context window. This design supports (i) resilience, allowing restarts on HPC resources following interruptions; (ii) inspectability, facilitating post hoc human review; and (iii) reproducibility, enabling packaging of the full evidence chain as Supporting Information. In this work, all demonstration are done with GPT-5.2-thinking-medium/high depending on the difficulty of the case.

CatMaster operates through a hierarchical loop comprising a Planner, an Executor, and a Summarizer, anchored by a persistent whiteboard record. Upon receiving a natural-language request, the Planner generates a structured milestone plan. The Executor carries out each task via specific tool calls and serializes the resulting artifacts to the workspace. The Summarizer then records outcomes as explicit updates to the whiteboard (e.g., UPSERT/DEPRECATE operations), tracking key facts, constraints, file pointers, and open questions at the end of each task and for the overall project. The system also supports human-in-the-loop checkpoints that are triggered when repeated tool failures or nonphysical outcomes are detected, allowing users to intervene at critical decisions while preserving the full audit trail.

## Tool layer for atomistic workflows

CatMaster integrates a domain-specific tool layer covering the essential operations of atomistic catalysis, including: (i) **Retrieval**: Search and download of bulk structures from the Materials Project;<sup>5</sup> (ii) **Construction**: Molecular building, slab generation, supercell creation, and selective dynamics constraints;<sup>1,2</sup> (iii) **Adsorption**: Symmetry-aware site enumeration and automated adsorbate placement; (iv) **Simulation**: Standardized VASP input preparation and batch job orchestration on HPC clusters;<sup>14-17</sup> (v) **Screening**: Surrogate model relaxations using MACE for high-throughput filtering;<sup>18</sup> and (vi) **Custom Logic**: Controlled Python execution for long-tail utilities. All tool inputs are validated against strict schemas to minimize parameter drift and ensure reproducibility.

## Computational settings and adaptive parameter generation

DFT calculations were prepared via the `relax_prepare` tool, which initializes VASP inputs from a robust baseline derived from a modified `MPRelaxSet` (via `pymatgen`). In the absence of explicit user constraints, CatMaster defaults to community-standard settings compatible with the Materials Project ecosystem. When additional constraints are specified, CatMaster preserves the baseline configuration while injecting targeted overrides to match the requested protocol (e.g., dispersion settings or selective-dynamics constraints).

Baseline parameters included a plane-wave cutoff of 520 eV, an electronic convergence threshold of `EDIFF=10-6` eV, and a force convergence criterion of `EDIFFG=-0.02` eV/Å. Spin polarization was enabled for magnetic systems.  $k$ -point meshes were generated automatically to maintain a consistent reciprocal-space density, with  $\Gamma$ -centered grids used for most bulk and slab calculations and  $\Gamma$ -only sampling used for large-box molecular calculations. Dispersion corrections (D3, `IVDW=11`) were enabled only when explicitly requested by the user or when required by a specified adsorption protocol. For surrogate screening, CatMaster utilized the pretrained MACE-MPA-0 model to perform rapid relaxations and energy ranking, reserving DFT calculations for targeted validation of shortlisted candidates.

For surrogate screening, CatMaster utilized the pretrained MACE-MPA-0 model as a multi-fidelity engine.<sup>18</sup> The agent employed the MACE model for rapid pre-relaxation and energy ranking, reserving DFT calculations for the validation of top-ranked candidates.

## Agent prompt overview

CatMaster employs a structured prompting strategy to manage planning, execution, and state updates. The core templates include:

- **Plan prompt:** decomposes a request into milestone tasks and returns a structured plan.
- **Plan-repair prompt:** corrects formatting when the plan does not satisfy schema

requirements.

- **Plan-feedback prompt:** revises the plan based on human feedback or tool constraints.
- **Task-execution prompt:** selects the next tool call or finalizes a task using the current whiteboard context and observations.
- **Task-summarization prompt:** aggregates task outcomes and emits explicit whiteboard update operations (e.g., UPSEERT/DEPRECATE).
- **Summarizer-repair prompt:** corrects whiteboard operations if schema validation fails.
- **Final-report prompt:** synthesizes a scientific report with references to workspace artifacts.

## Thermodynamic definitions

Surface energies ( $\gamma$ ) were computed from relaxed symmetric slabs according to:

$$\gamma = \frac{E_{\text{slab}} - NE_{\text{bulk}}}{2A}, \quad (1)$$

where  $E_{\text{slab}}$  is the total energy of the slab,  $E_{\text{bulk}}$  is the energy per atom of the relaxed bulk,  $N$  is the number of atoms in the slab, and  $A$  is the surface area of one face.

Adsorption energies ( $E_{\text{ads}}$ ) were defined as:

$$E_{\text{ads}} = E(\text{slab+ads}) - E(\text{slab}) - E(\text{ads}), \quad (2)$$

where  $E(\text{ads})$  refers to the energy of the isolated adsorbate in a vacuum box.

For HER screening, the free energy of hydrogen adsorption was approximated following

the standard computational hydrogen electrode (CHE) model:<sup>19</sup>

$$\Delta E_{H^*} = E(\text{slab+H}) - E(\text{slab}) - \frac{1}{2}E(\text{H}_2), \quad (3)$$

$$\Delta G_{H^*} = \Delta E_{H^*} + 0.24 \text{ eV}, \quad (4)$$

where the 0.24 eV term accounts for the zero-point energy (ZPE) and entropic contributions at 298.15 K as an empirical value.

## Acknowledgement

This work was supported by the National Key R&D Program of China (No. 2022ZD0117501), the Scientific Research Innovation Capability Support Project for Young Faculty (ZYGXQN-JSKYCXNLZCXM-E7), the Tsinghua University Initiative Scientific Research Program, and the Carbon Neutrality and Energy System Transformation (CNEST) Program led by Tsinghua University.

## Supporting Information Available

The source code for reproducing this work is available at <https://github.com/q734738781/CatMaster>. Archived workspaces for the demonstrations presented in this manuscript are distributed alongside the code in the repository under the `demos/` directory.

## References

- (1) Larsen, A. H.; Mortensen, J. J.; Blomqvist, J.; Castelli, I. E.; Christensen, R.; Dułak, M.; Friis, J.; Groves, M. N.; Hammer, B.; Hargus, C.; others The atomic simulation environment—a Python library for working with atoms. *Journal of Physics: Condensed Matter* **2017**, *29*, 273002.

(2) Ong, S. P.; Richards, W. D.; Jain, A.; Hautier, G.; Kocher, M.; Cholia, S.; Gunter, D.; Chevrier, V. L.; Persson, K. A.; Ceder, G. Python Materials Genomics (pymatgen): A robust, open-source python library for materials analysis. *Computational Materials Science* **2013**, *68*, 314–319.

(3) Jain, A.; Ong, S. P.; Chen, W.; Medasani, B.; Qu, X.; Kocher, M.; Brafman, M.; Petretto, G.; Rignanese, G.-M.; Hautier, G.; others FireWorks: a dynamic workflow system designed for high-throughput applications. *Concurrency and Computation: Practice and Experience* **2015**, *27*, 5037–5059.

(4) Pizzi, G.; Cepellotti, A.; Sabatini, R.; Marzari, N.; Kozinsky, B. AiiDA: automated interactive infrastructure and database for computational science. *Computational Materials Science* **2016**, *111*, 218–230.

(5) Jain, A.; Ong, S. P.; Hautier, G.; Chen, W.; Richards, W. D.; Dacek, S.; Cholia, S.; Gunter, D.; Skinner, D.; Ceder, G.; others Commentary: The Materials Project: A materials genome approach to accelerating materials innovation. *APL materials* **2013**, *1*.

(6) Zou, Y.; Cheng, A. H.; Aldossary, A.; Bai, J.; Leong, S. X.; Campos-Gonzalez-Angulo, J. A.; Choi, C.; Ser, C. T.; Tom, G.; Wang, A.; others El Agente: An autonomous agent for quantum chemistry. *Matter* **2025**, *8*.

(7) Pham, T. D.; Tanikanti, A.; Keçeli, M. ChemGraph as an agentic framework for computational chemistry workflows. *Communications Chemistry* **2026**,

(8) Wang, Z.; Huang, H.; Zhao, H.; Xu, C.; Zhu, S.; Janssen, J.; Viswanathan, V. DREAMS: Density functional theory based research engine for agentic materials simulation. *arXiv preprint arXiv:2507.14267* **2025**,

(9) Rothfarb, S.; Davis, M. C.; Matanovic, I.; Li, B.; Holby, E. F.; Kort-Kamp, W. J.

Hierarchical Multi-agent Large Language Model Reasoning for Autonomous Functional Materials Discovery. *arXiv preprint arXiv:2512.13930* **2025**,

- (10) Liu, J.; Zhu, T.; Ye, C.; Fang, Z.; Weng, H.; Wu, Q. VASPilot: MCP-facilitated multi-agent intelligence for autonomous VASP simulations. *Chinese Physics B* **2025**, *34*, 117106.
- (11) The VASP Team Atoms and Molecules. <https://www.vasp.at/tutorials/latest/molecules/part1/>, 2024; Accessed: 2026-01-18.
- (12) Heiniger, N. M. A first-principle study of the surface energy of FeCrAl alloys. 2025.
- (13) Tan, X.; Zhou, J.; Peng, Y. First-principles study of oxygen adsorption on Fe (1 1 0) surface. *Applied surface science* **2012**, *258*, 8484–8491.
- (14) Kresse, G.; Furthmüller, J. Efficient iterative schemes for ab initio total-energy calculations using a plane-wave basis set. *Physical review B* **1996**, *54*, 11169.
- (15) Kresse, G.; Furthmüller, J. Efficiency of ab-initio total energy calculations for metals and semiconductors using a plane-wave basis set. *Computational materials science* **1996**, *6*, 15–50.
- (16) Kresse, G.; Joubert, D. From ultrasoft pseudopotentials to the projector augmented-wave method. *Physical review b* **1999**, *59*, 1758.
- (17) Yuan, F.; Ding, Z.; Liu, Y.-P.; Cao, K.; Fan, J.; Nguyen, C. T.; Zhang, Y.; Wang, H.; Chen, Y.; Huang, J.; others DPD Dispatcher: Scalable HPC Task Scheduling for AI-Driven Science. *Journal of Chemical Information and Modeling* **2025**, *65*, 12155–12160.
- (18) Batatia, I.; Benner, P.; Chiang, Y.; Elena, A. M.; Kovács, D. P.; Riebesell, J.; Advincula, X. R.; Asta, M.; Avaylon, M.; Baldwin, W. J.; others A foundation model for atomistic materials chemistry. *arXiv preprint arXiv:2401.00096* **2023**,

(19) Nørskov, J. K.; Bligaard, T.; Logadottir, A.; Kitchin, J.; Chen, J. G.; Pandelov, S.; Stimming, U. Trends in the exchange current for hydrogen evolution. *Journal of The Electrochemical Society* **2005**, *152*, J23.